Exploration of Resting State Networks in Human Cervical Spinal Cord

Xiaojia Liu[1,2], Xiang Li[2], Fuqing Zhou[2], Jiaolong Cui[2], Adrian Tsang[1,3], Iris Y. Zhou[1,3], Ed X. Wu[1,3], and Yong Hu[2]

[1]*Laboratory of Biomedical Imaging and Signal Processing, The University of Hong Kong, Hong Kong, China,* [2]*Department of Orthopaedics and Traumatology, The University of Hong Kong, Hong Kong, China,* [3]*Department of Electrical and Electronic Engineering, The University of Hong Kong, Hong Kong, China*

INTRODUCTION: Resting state fMRI (rsfMRI) has gained wide interests to investigate the correlation among brain regions based on spontaneous fluctuating low frequency BOLD signals [1-3]. But few rsfMRI studies have explored functional connectivity in human spinal cord [4-6]. The distribution of resting state BOLD signals over the slices (from vertebra C3 to C5 or from vertebra C5 to vertebral T1) was reported in previous studies [4, 6]. However, the resting state network (RSN) maps described in these studies were only subject-specific. There has been no report to date on group-based RSN analysis. In this study, we aim to detect the group averaged RSN in the human cervical spinal cord using rsfMRI.

METHODS: Data acquisition & participants: Fourteen healthy subjects (Female/Male = 5/9, age = 33±4 years) were imaged in this study using a 3T Philips Achieva whole body MRI scanner and a 33-channel head spine coil. The rsfMRI images were acquired using a gradient echo EPI sequence with parameters as follows: TR/TE = 2000/30 ms, Flip Angle = 50^0, Number of Slices = 26, voxel size = 1.25x1.25x4 mm, FOV = 80x80x104 mm (from vertebrae C1 to C7).

Image processing: The raw EPI images were processed using SPM8 and REST toolboxes in MATLAB for slice timing, motion correction, detrend, and band-pass filtering between 0.01 and 0.08Hz. The first 10 volumes were deleted to remove the initial transient effects.

Masks were manually drawn over the gray matter on 15 out of 26 slices covering from C2 to C6 segments (3 slices for each segment) (Figure 1A). The slices crossing C1, C7 segments and intervertebral discs, were not masked due to FOV mismatch or severe artifact. Each gray matter mask was separated into ventral horn and dorsal horn (Figure 1B) due to their different involvement in neural activity (ventral horn controls motor and dorsal horn controls sensory). Thirty regions of interest (ROI) were depicted in total (5 segments, 3 slices per segment, and 2 masks per slice). The ROIs that delineated the ventral horn and dorsal horn from C2 to C6 segments were numbered sequentially from 1 to 30. Since BOLD fluctuation mainly happens in the neurons of gray matter, power spectrum density of signals inside and outside the gray matter masks were calculated to check the accuracy of ROIs placement (Figure 1C).

ROI-based functional correlation analysis: Functional correlation was calculated using REST toolbox in MATLAB between pairs of ROIs to obtain a 30x30 correlation matrix for each subject and subsequently generate the mean correlation coefficient (CC) map. Fisher Z-transformation was performed in each correlation matrix. One-sample t-test was performed to test the correlation significance with false discovery rate (FDR) correction. Group RSN analysis was based on the Z-transformed matrices from all subjects.

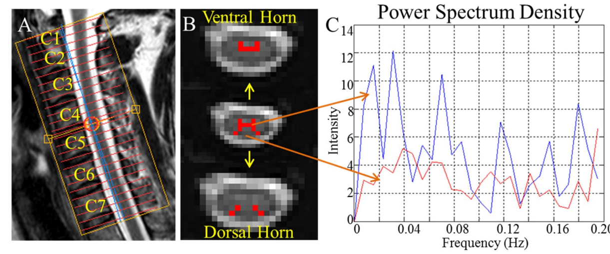

Figure 1 The FOV and slices location that cover vertebra C1 to C7 (A); ROI placement to delineate ventral horn and dorsal horn drawn on post-processed EPI images (B); power spectrum density comparison between BOLD signal inside and outside the gray matter mask (C)

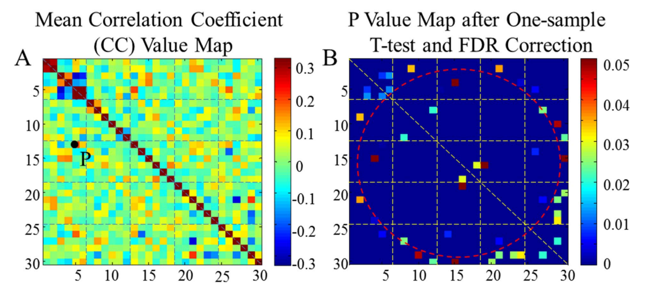

Figure 2 Mean correlation coefficient (CC) map calculated from ROI correlation analysis result from all subjects, the diagonal line is the axis of symmetry, points on diagonal line are CC values between the same ROI (A); p value map of one-sample t-test after FDR correction and points with significant correlation ($p<0.05$) are shown (B); The coordinate 1-30 stands for ventral horn and dorsal horn of each slice on segments from C2 to C6 sequentially. For example, in Figure 2A the coordinate of point P is (13, 5) and that shows the correlation information between ventral horn on slice 1 of C4 segment and ventral horn on slice 3 of C2 segment.

RESULTS: The 30x30 symmetric matrix of mean correlation coefficient (CC) value map generated from all subjects is shown in Figure 2A. Each point represents the mean correlation coefficient between two ROIs and the diagonal line is the axis of symmetry in the figures. Points on the diagonal line represent correlation between the same ROI, whose CC value is 1. The coordinate label (1-30) represents ROIs of ventral horn and dorsal horn on each slice segment from C2 to C6. Figure 2B shows the p value map of the result from the one-sample t test after FDR correction, where only points with significant differences ($p<0.05$) are shown. Interestingly, most of the points with significant correlation were located around the circle, which revealed that C2 and C6 segments have stronger correlations with other segments. In contrast, few pair of ROIs with significant correlation was found on the segments of C3, C4 and C5. The significant correlation coefficient (FDR corrected $p<0.05$) was summarized in Table 1. We found that C2 segment also has a stronger inter-segment correlation than other segments.

Table 1 Significant Correlation ROI Pairs

ROI pair	CC value	p value
C2 slice 2 VH - **C2** slice 3 VH	-0.279	0.008
C2 slice 2 VH - **C2** slice 3 DH	-0.231	0.013
C2 slice 3 VH - **C2** slice 3 DH	0.322	0.012
C2 slice 1 DH - C3 slice 2 VH	-0.111	0.034
C2 slice 2 DH - C4 slice 2 VH	0.158	0.049
C2 slice 1 DH - C5 slice 2 VH	0.139	0.036
C2 slice 2 DH - C5 slice 3 DH	0.128	0.004
C2 slice 3 VH - **C6** slice 1 DH	0.179	0.005
C3 slice 1 DH - C3 slice 3 DH	-0.114	0.021
C4 slice 2 DH - C4 slice 3 DH	0.161	0.029
C4 slice 2 DH - C5 slice 1 VH	0.102	0.049
C3 slice 1 DH - **C6** slice 2 VH	0.142	0.025
C3 slice 2 DH - **C6** slice 3 VH	0.093	0.047
C3 slice 3 DH - **C6** slice 3 DH	-0.115	0.023
C4 slice 1 DH - **C6** slice 1 VH	-0.193	0.007
C4 slice 2 VH - **C6** slice 3 DH	0.061	0.049
C5 slice 1 DH - **C6** slice 3 DH	-0.104	0.026
C5 slice 2 VH - **C6** slice 2 VH	-0.273	0.006
C5 slice 2 VH - **C6** slice 3 VH	0.208	0.025
C5 slice 3 VH - **C6** slice 3 VH	-0.192	0.026
C5 slice 3 DH - **C6** slice 3 VH	-0.163	0.032
C6 slice 2 VH - **C6** slice 3 VH	-0.171	0.021

Note: VH = ventral horn; DH = dorsal horn; CC = correlation coefficient. It's clear that C2 and C6segment have much higher appearance rate than other segments in Table 1.

DISCUSSION AND CONCLUSION: In this study, the correlation between ventral or dorsal horn of gray matter at different segments was investigated. The results are consistent with previous studies in which RSN maps were generated from independent component analysis [4] and seed-based correlation approach [6]. However, these previous studies only presented RSN maps at individual level. To the best of our knowledge, this is the first demonstration of group-based mean RSN in the human cervical spinal cord. The C2 and C6 segments showed more functional connectivity with other segments, which indicated both C2 and C6 acted as 'hubs' of neural activity in the spinal cord. Our finding may suggest that the functional connectivity analysis of the human cervical spinal cord using rsfMRI could be a promising tool to further investigate the physiological function of spinal cord as well as the underlying pathophysiology of spinal cord in trauma and degenerative conditions.

REFERENCES: [1] Smith S M, Fox P T, Miller K L, et al. Proc Natl Acad Sci U S A., 2009, 106(31): 13040-13045. [2] Raichle M E. Brain Connect. 2011, 1(1): 3-12. [3] Fox M D, Raichle M E. Nat Rev Neurosci, 2007, 8(9): 700-711. [4] Barry R L, Smith S A, Gore J C, Proc. Intl. Soc. Mag. Reson. Med. 21 (2013); 2237. [5] Barry R L, Gore H C, Smith S A, Proc. Intl. Soc. Mag. Reson. Med. 21 (2013); 2278. [6] Wei, Pengxu, et al. Eur J Appl Physiol 108.2 (2010): 265-271.